

## Research Article

# MU-MIMO in LTE Systems

**Jonathan Duplicy,<sup>1</sup> Biljana Badic,<sup>2</sup> Rajarajan Balraj,<sup>2</sup> Rizwan Ghaffar,<sup>3</sup>  
Péter Horváth,<sup>4</sup> Florian Kaltenberger,<sup>3</sup> Raymond Knopp,<sup>3</sup> István Z. Kovács,<sup>5</sup>  
Hung T. Nguyen,<sup>6</sup> Deepaknath Tandur,<sup>1</sup> and Guillaume Vivier<sup>7</sup>**

<sup>1</sup>Agilent Technologies Laboratories, Wingepark 51, 3110 Rotselaar, Belgium

<sup>2</sup>Intel Mobile Communications (IMC), Düsseldorf Landstraße 401, 47259 Duisburg, Germany

<sup>3</sup>Eurecom, 2229 route des Crêtes, B.P. 193, 06904 Sophia Antipolis Cedex, France

<sup>4</sup>Department of Broadband Infocommunications, Budapest University of Technology and Economics, Goldmann György tér 3., 1111 Budapest, Hungary

<sup>5</sup>Nokia Siemens Networks Denmark A/S, Niels Jernes Vej 10, 9220 Aalborg, Denmark

<sup>6</sup>Department of Electronics Systems, Aalborg University, Niels Jernes Vej 12, 9220 Aalborg, Denmark

<sup>7</sup>Sequans Communications, Le Parvis de La Défense 19, 92 073 Paris La Défense Cedex, France

Correspondence should be addressed to Jonathan Duplicy, jonathan\_duplicy@agilent.com

Received 1 December 2010; Revised 2 February 2011; Accepted 8 March 2011

Academic Editor: Rodrigo C. De Lamare

Copyright © 2011 Jonathan Duplicy et al. This is an open access article distributed under the Creative Commons Attribution License, which permits unrestricted use, distribution, and reproduction in any medium, provided the original work is properly cited.

A relatively recent idea of extending the benefits of MIMO systems to multiuser scenarios seems promising in the context of achieving high data rates envisioned for future cellular standards after 3G (3rd Generation). Although substantial research has been done on the theoretical front, recent focus is on making Multiuser Multiple-Input Multiple-Output (MUMIMO) practically realizable. This paper presents an overview of the different MU-MIMO schemes included/being studied in 3GPP standardization from LTE (long-term evolution) to LTE Advanced. MU-MIMO system concepts and implementation aspects have been studied here. Various low-complexity receiver architectures are investigated, and their performance assessed through link-level simulations. Appealing performance offered by low-complexity interference aware (IA) receivers is notably emphasized. Furthermore, system level simulations for LTE Release 8 are provided. Interestingly, it is shown that MU-MIMO only offers marginal performance gains with respect to single-user MIMO. This arises from the limited MU-MIMO features included in Release 8 and calls for improved schemes for the upcoming releases.

## 1. Introduction

Wireless data usage is increasing faster now than ever before. Smartphones and broadband-enabled portables, such as laptops or tablets, are now seeing high penetration in many markets, and the superior user experience offered by such devices has led to exponential growth of mobile data traffic as shown in [1]. The demand for mobile data services has increased by an average of 160% in the year 2009 alone, and some mobile carriers have experienced even more aggressive growth numbers. According to a recent forecast, the global mobile data traffic is expected to continue to double every year through 2014, leading to a global compound annual growth rate of 108% [2].

These large capacity demands can be met only by highly efficient and optimized mobile network infrastructures. Significant improvements are expected with the ongoing roll-out of OFDMA- (Orthogonal Frequency Division Multiple Access-) based networks: IEEE 802.16x (WiMAX) and 3GPP (3rd generation partnership project) LTE. These two standards, although they do not fulfill the requirements, are the first steps towards the 4th generation (4G) definition given by the International Telecommunications Union (ITU) and targeting data rates of 100 Mbps in high-mobility applications and 1 Gbps for low-mobility applications such as nomadic/local wireless access.

To meet these needs, advanced features are investigated for inclusion in future releases of these standards (WiMAX

evolution and LTE Advanced). Among these various techniques, two promising ones are currently being investigated by EU FP7 project SAMURAI (Spectrum Aggregation and Multiuser MIMO: ReAl-World Impact) [3], namely, carrier aggregation and MU-MIMO. The main objective of SAMURAI project is to investigate innovative techniques in the area of MU-MIMO and SA with focus on practical implementation and deployment aspects.

This paper aims at giving an insight into MU-MIMO schemes included/being studied in 3GPP releases. MU-MIMO concepts, fundamentals, and an overview of already published research results and current outcomes from SAMURAI project are shown in this paper. Specifically, Section 2 provides a detailed overview of the different MU-MIMO schemes from LTE Release 8 to Release 10 (known as LTE Advanced). In addition, a novel scheduling algorithm based on the geometrical alignment of interference at the base station which minimizes the effective interference seen by each user equipment (UE) is shown. In Section 3, receiver design for MU-MIMO is addressed. The performance of both interference unaware and interference aware (IA) types of receiver algorithms has been studied in an LTE downlink system. Performance/complexity tradeoff is summarized. System level simulations are provided in Section 4, and gains offered by MU-MIMO schemes with respect to single-user MIMO (SU-MIMO) schemes in LTE Release 8 are emphasized. Finally, conclusions are given in Section 5.

Regarding notations, we will use lowercase or uppercase letters for scalars, lowercase boldface letters for vectors, and uppercase boldface letters for matrices. Furthermore,  $|\cdot|$  and  $\|\cdot\|$  indicate the norm of scalar and vector while  $(\cdot)^T$ ,  $(\cdot)^*$ , and  $(\cdot)^\dagger$  stand for the transpose, conjugate, and conjugate transpose, respectively.

## 2. Overview of MU-MIMO in 3GPP Standards

**2.1. Theoretical Foundations of MU-MIMO.** Spatial dimension surfacing from the usage of multiple antennas promises improved reliability, higher spectral efficiency, and spatial separation of users. This spatial dimension is particularly beneficial for precoding in the downlink of MU cellular system, where spatial resources can be used to transmit data to multiple users simultaneously. The MIMO transmission techniques are integral parts of the LTE and WiMAX standards. A good overview of the MIMO techniques and configuration supported in these radio access technologies can be found in [4–7].

In MU-MIMO mode, the transmissions to several terminals are overlapped in the same time-frequency resources by exploiting the spatial diversity of the propagation channel. In order to fully exploit MU-MIMO transmission modes, the spatial streams intended to the targeted terminals need to be well separated, ideally orthogonal at both transmit and receive sides. As a consequence, the theoretical performance gain of the MU-MIMO over SU-MIMO is expected to significantly increase in spatially correlated channels and with increasing number of transmit antenna at the enhanced Node B (eNB). Various linear and nonlinear precoding techniques and the corresponding receiver structures have

been proposed in the literature in order to achieve promising MU-MIMO gains, see, for example, [8–12].

Optimal precoding in MU-MIMO Gaussian broadcast channel involves a theoretical preinterference subtraction technique known as dirty paper coding (DPC) [10] combined with an implicit user scheduling and power loading algorithm. Linear precoding techniques such as channel inversion (CI) [11] and regularized channel inversion (RCI) [12] cancel the interference in the former case while attenuating it in the latter case. These precoding strategies strive to transform the cross-coupled channels into parallel noninteracting channels therefore transforming MU downlink into parallel SU systems. They are assuming Gaussianity of the interference. However, in the real world, inputs must be drawn from discrete constellations which have (non-Gaussian) structures that can be exploited in the detection process.

For practical purposes, the derived theoretical solutions have to be further adapted to the requirements and restrictions of standardized air interfaces. The following sections summarize some of the critical physical layer design aspects.

### 2.2. Overview of 3GPP LTE PHY MIMO

**2.2.1. Reference Signals.** The downlink transmission schemes are supported at physical layer by a set of downlink reference signals. These reference signals can be either UE specific or cell specific. The latter are referred to as common reference signals (CRSs) while the former are referred to as dedicated (or demodulation) reference signals (DRSs or DM-RSs). The CRSs are not precoded signals and are used by the UE for channel estimation, while the DM-RSs are precoded and used for demodulation purposes on the scheduled physical resource blocks (PRBs). The 3GPP standard defines the transmission of one time-frequency pattern for CRS and DM-RS assigned to one real or virtual *antenna port*.

**2.2.2. Transmission Modes.** The defined SIMO (Single-Input Multiple-Output) and MIMO transmission schemes are categorized in several *transmission modes*. The definition of each transmission mode includes the required configuration information in the common downlink signaling channel and information on how the user terminal should search for this configuration message [13]. This mechanism is part of the general downlink signaling framework designed to allow a flexible time-frequency resource allocation separately to each UE based on the available system resources and the reported or measured channel conditions. The transmission mode for each UE is configured semistatically via higher layer signaling, in order to avoid excessive downlink signaling.

**2.2.3. Precoding.** A major prerequisite for SU- and MU-MIMO transmission schemes is the use of precoding mechanisms at the transmit side. In 3GPP LTE/LTE Advanced, different codebooks have been defined depending on the number of transmit antenna ports, and they provide precoding support for simultaneous transmission of variable number of layers (data stream) to the same target UE [4–7, 13].

The precoding is applied to the data transmission to a target UE based on the channel feedback received from that UE, including a channel rank indicator (RI), channel quality indicator (CQI), and precoding matrix indicator (PMI). The RI indicates the estimated number of simultaneous layers which can be received by the UE. One or more layers can be mapped to the same *codeword* and are jointly encoded for transmission to the same target UE. The RI is estimated at the UE as a wideband measure, that is, the same channel rank is assumed on all allocated resources. The CQI is an index in the modulation coding scheme (MCS) and transport block size (TBS) index table (32 different entries). The PMI is an index in the codebooks defined for a given number or transmit antenna ports (1, 2, 4 in LTE and up to 8 for LTE Advanced). The CQI information is always derived under the assumption that the selected PMI will be applied to the next scheduled transmission. A more detailed analysis of the LTE MU-MIMO precoding mechanisms and codebook use is presented in Section 2.6.

**2.2.4. Signalling and Terminal Feedback.** The physical layer procedures defined for LTE Release 8 support various mechanisms of controlling the transmission parameters with both higher-layer and lower-layer signaling [13, 14]. The time-frequency granularity of the feedback to be sent by the UE is configured by the network via the downlink signaling channel and scheduling grants. Certain restrictions apply mainly due to requirement of minimizing the downlink and uplink signaling overheads. In practice, this means that each of the defined *transmission modes* supports a certain limited set of physical layer transmission schemes and feedback schemes.

There are two main categories of CQI/PMI feedback mechanisms defined in the time domain: periodic and aperiodic. The RI is always a frequency nonselective type feedback and is associated with the corresponding CQI/PMI feedback. The supported time-frequency CQI/PMI feedback granularities determine the overall feedback amount, and the supported configurations depend on the physical uplink channel utilized. The aperiodic feedback—frequency selective—is supported on the uplink shared channel and is available only when the UE has downlink/uplink transmission scheduled while for the periodic feedback—frequency non/selective—both uplink control and shared channels can be used [13].

**2.3. LTE Release 8.** The first release of LTE (Release 8) was aimed at defining the new OFDMA-based air-interface and introduced advanced single-user MIMO transmission schemes, which were evaluated to be sufficient to meet the set performance targets [4–7, 15]. Transmission from up to four antenna ports is supported. The spatial multiplexing or diversity MIMO transmission schemes, that is, including MU-MIMO, use only the nonprecoded CRS while the precoded DRS can support single-user single-layer beamforming schemes.

In LTE Release 8 there is only one transmission mode defined which allows, for MU-MIMO scheme to be used,

TABLE 1: CQI and PMI feedback types for transmission mode 5 in LTE.

Feedback	CQI type	PMI type
Aperiodic	Higher-layer configured, set of subbands: subband and wideband CQI per codeword	Single PMI
Periodic	Wideband CQI for first codeword spatial differential CQI for RI > 1	Single PMI
Periodic	UE-selected subbands: full CQI for first codeword spatial differential CQI for RI > 1	Single PMI

the *transmission mode 5* (TM5). When configured in TM5, the UE assumes that the eNB transmission on the downlink shared channel is performed with a single layer (stream). For the case of two transmit antenna ports, the standard specifies the use of four precoders based on two bits feedback from the UEs. In the case of four transmit antenna ports, the number of precoders increases to sixteen, which can be found in [16].

The downlink control information (DCI) format used for TM5 is format 1D, which includes a 1-bit power offset information, indicating whether a 3 dB transmit power reduction should be assumed or not.

In terms of terminal feedback and CQI/PMI reporting modes, the LTE MU-MIMO TM5 can use both aperiodic and periodic feedback types, see Table 1. When aperiodic reporting is configured, then the wideband CQI and higher layer selected subband CQI in combination with a single PMI is supported. The full CQIs are reported for each codeword. When periodic reporting is configured then either wideband CQI or UE-selected subband CQI in combination with a single PMI is supported. The full CQI is reported for the first codeword only, and differential CQI is used for the second codeword when the reported RI > 1. Single (or wideband) PMI means that the reported PMI corresponds to and assumes transmission on all selected subbands reported for the CQI(s) and RI.

This is a rather minimal MU-MIMO transmission scheme and relies heavily on the accuracy of the RI/CQI/PMI feedback which was optimized for SU-MIMO transmission schemes. Inevitably, this limits the achievable MU-MIMO performance.

**2.4. LTE Release 9.** In the second release of LTE (Release 9), new support has been added for the transmission modes utilizing virtual antenna ports with precoded UE-specific reference signals. The DRS has been extended to two additional antenna ports. Code division multiplexing is used to orthogonalize the transmission on the two new virtual antenna ports, while nonorthogonal scrambling codes are introduced to support dual-layer transmission on each of the antenna ports. This new dual-layer transmission mode is targeted for beamforming schemes and supports MU-MIMO transmission for up to 4 UEs rank 1 (orthogonal) or up to 2 UEs rank 2 (non-orthogonal). However, the antenna

port and scrambling code allocations are wideband, so it is not always possible to ensure orthogonality even when only 2 users are multiplexed in MU-MIMO mode. Furthermore, the only fall-back transmission mode which is supported, without mode reconfiguration, is the transmit diversity. A fully adaptive SU/MU-MIMO transmission mode is not supported in LTE Release 9 but is expected to be introduced in Release 10 as described in the next section.

*2.5. LTE Advanced.* The specifications of LTE have been extended for LTE Advanced [17]. At the time of writing, the specifications had not been finalized, but several details are already in place. The final specifications are expected to be frozen in March 2011.

Configurations with up to  $8 \times 8$  MIMO are to be supported, and new reference signals have been introduced to support both demodulation of the DM-RS and channel state information estimation (CSI-RS). Hence, special attention has been given to the signaling needed for more advanced SU/MU-MIMO schemes. A new transmission mode has been defined which now includes both SU and MU-MIMO transmission capabilities without the need for the UEs to be reconfigured via higher-layer signaling when switching between SU and MU transmission/reception on the shared data channel [18]. This is the *transmission mode 9* (TM9).

Consequently, the set of precoding codebooks has been also extended for LTE Advanced [19]. For configuration with 2- and 4-transmit antenna, the LTE-Advanced codebook is the same as the corresponding LTE codebooks. For configurations with 8-transmit antenna, a dual-codebook approach is used. The precoding to be used in the dual-codebook approach is obtained via multiplication of two precoding matrices  $W_1$  and  $W_2$ , where  $W_1$  is block diagonal matrix matching the spatial covariance matrix of dual-polarized antenna setup, and  $W_2$  is the antenna selection and cophasing matrix. This configuration provides good performance in both high and low spatial correlation channels. The  $W_1$  are obtained from the coefficients of a Digital Fourier Transform (DFT) corresponding to different transmission ranks, see Table 2, with details in [19].

Backwards compatibility for Release 8 and 9 UEs has been targeted. This means that many of the LTE-Advanced features and associated signaling are not visible for the Release 8 and 9 UEs, and the transmission schemes defined for LTE are fully supported.

The UE feedback definition has been also extended in LTE Advanced to account for the dual-codebook structure. When operating in a cell with 8-transmit antenna configuration, the LTE-Advanced UEs are required to include in the feedback information the PMI corresponding to both  $W_1$  and  $W_2$ . When only 2- or 4-transmit antenna are configured/used at the eNB, the feedback includes only the PMI for  $W_2$ , and the  $W_1$  is the identity matrix. Furthermore, the aperiodic CQI/PMI reporting schemes defined for LTE have been extended to support the dual codebook [20]. The PMI for  $W_1$  is always reported as a wideband PMI corresponding to the entire system bandwidth. The aperiodic feedback modes include the configurations with

TABLE 2: Codebook design in LTE Advanced for 8-transmit antenna.

Tx rank	Beams	$W_1$	$W_2$
Rank 1-2	32	16 (per rank)	16 (per rank)
Rank 3-4	16	4 (per rank)	16 (rank 3), 8 (rank 4)
Rank 5-7	1	4	1 (per rank)
Rank 8	1	1	1 (per rank)

wideband CQI-subband PMI  $W_2$ , wideband + “Best-M” CQI-wideband + “Best-M” PMI  $W_2$ , and subband CQI-wideband PMI  $W_2$ .

At this stage, not all LTE-Advanced MIMO specifications have been finalized, and there are still several open aspects to be addressed. Proposals to improve the CQI/PMI feedback also for 2- and 4-transmit antenna configurations, targeting both MU-MIMO and SU-MIMO improvement, are yet to be considered. Similar to the LTE Release 8 and 9 design principles, these further improvements have to take the performance versus signaling overhead tradeoff into account even when utilizing the new transmission mode introduced in LTE Advanced. The natural extensions of the RI/CQI/PMI feedback periodic and aperiodic reporting schemes already defined in LTE are to be further investigated in this context.

*2.6. Optimal Precoding Strategy for LTE Release 8.* The LTE Release 8 precoders are of low resolution and are further based on the principle of equal gain transmission (EGT). As these precoders have been designed for SU-MIMO transmission, their efficient employment for MU-MIMO mode (TM5) is not yet fully understood. This has led to the common perception that MU-MIMO is not workable in LTE [21, page 244]. In this section, we investigate the effectiveness of these low-resolution precoders for MU-MIMO mode in LTE and consider a geometric scheduling algorithm which outperforms SU-MIMO and transmit diversity schemes. This algorithm is based on the geometrical alignment of interference at eNB which minimizes the effective interference seen by each UE.

*2.6.1. System Model.* We restrict ourselves to the case of dual-antenna eNB and single-antenna UEs. The system equation for LTE TM5 at the  $k$ -th resource element (RE) is given as

$$y_{1,k} = \mathbf{h}_{1,k}^\dagger \mathbf{p}_{1,k} x_{1,k} + \mathbf{h}_{1,k}^\dagger \mathbf{p}_{2,k} x_{2,k} + z_{1,k}, \quad (1)$$

where  $y_{1,k}$  is the received symbol at UE-1, and  $z_{1,k}$  is the zero mean circularly symmetric complex white Gaussian noise of variance  $N_0$ .  $x_{1,k}$  and  $x_{2,k}$  are the complex symbols for UE-1 and UE-2, respectively.  $\mathbf{h}_{1,k}^\dagger = [h_{11,k}^* \quad h_{21,k}^*]$  symbolizes the MISO channel from eNB to UE-1 at the  $k$ -th RE. Since the processing at UE is assumed to be performed on an RE basis for each received OFDM symbol, the dependency on RE index can be ignored for notational convenience.

*2.6.2. PMI Calculation.* As the decision to schedule an UE in one of the transmission modes will be made by eNB,

each UE would feedback the precoder which maximizes its received signal strength. Therefore, in accordance with the low-resolution LTE precoders, the UEs compute quantized versions of their respective matched filter (MF) precoders, that is, the UE first measures its channel  $\mathbf{h}_1^\dagger = [h_{11}^* \quad h_{21}^*]$  from eNB and consequently computes the MF precoder, that is,  $[h_{11} \quad h_{21}]^T$  (the normalized version involves a division by  $\|\mathbf{h}_1\|$ ). As LTE precoders are characterized by unit coefficients as their first entry, the UE normalizes first coefficient of the MF precoder, that is,

$$\mathbf{p}_{\text{MF}} = \frac{h_{11}^*}{|h_{11}|^2} \begin{bmatrix} h_{11} \\ h_{21} \end{bmatrix} = \begin{bmatrix} 1 \\ \frac{h_{11}^* h_{21}}{|h_{11}|^2} \end{bmatrix}. \quad (2)$$

Second coefficient indicates the phase between two channel coefficients. Now based on the minimum distance between  $\mathbf{p}_{\text{MF}}$  and LTE precoders, one of the four precoders is selected by the UE, and the index of that precoder is fed back to the eNB. Let that precoder be  $\mathbf{p}_1 = [1 \quad q]^T$ ,  $q \in \{\pm 1, \pm j\}$ . From the geometrical perspective, this precoder once employed by the eNB would align  $h_{21}^*$  with  $h_{11}^*$  in the complex plane so as to maximize the received signal power, that is,  $|h_{11}^* + qh_{21}^*|^2$  subject to the constraint that the precoder allows rotation of  $h_{21}^*$  by  $0^\circ$ ,  $\pm 90^\circ$ , or  $180^\circ$ . Therefore, this precoding ensures that  $h_{11}^*$  and  $h_{21}^*$  lie in the same quadrant as shown in Figure 1(b), thus maximizing the received SNR.

**2.6.3. Scheduling.** In LTE MU-MIMO mode (TM5), dual antenna eNB can serve two UEs on the same time-frequency resources. We assume a densely populated cell where eNB has the requested precoders of most of the UEs in the cell. Here, we consider a scheduling algorithm for MU-MIMO mode where eNB selects the second UE in each group of allocatable RBs whose requested precoder  $\mathbf{p}_2$  is  $180^\circ$  out of phase from the precoder  $\mathbf{p}_1$  of the first UE to be served on the same RBs, that is, the precoder matrix is given as  $\mathbf{P} = 1/\sqrt{4} \begin{bmatrix} 1 & 1 \\ q & -q \end{bmatrix}$ . So the received signal by UE-1 is given as

$$y_1 = \frac{1}{\sqrt{4}}(h_{11}^* + qh_{21}^*)x_1 + \frac{1}{\sqrt{4}}(h_{11}^* - qh_{21}^*)x_2 + z_1, \quad (3)$$

where selection of the precoder for each UE would ensure maximization of its desired signal strength, that is,  $|\mathbf{h}_1^\dagger \mathbf{p}_1|^2$  for the first UE and  $|\mathbf{h}_2^\dagger \mathbf{p}_2|^2$  for the second UE while selection of the UE pairs with out-of-phase precoders would ensure minimization of the interference strength seen by each UE, that is,  $|\mathbf{h}_1^\dagger \mathbf{p}_2|^2$  for the first UE and  $|\mathbf{h}_2^\dagger \mathbf{p}_1|^2$  for the second UE. Note that these maximization and minimization are subject to the constraint of the utilization of low-resolution LTE precoders. This scheduling strategy would ensure that the UEs selected to be served in MU-MIMO mode on the same time-frequency resources have good channel separation.

Though this precoding and scheduling strategy would ensure minimization of the interference, the residual interference would still be significant due to the low resolution of LTE precoders. The employment of single-user receivers

by the UEs (thereby assuming Gaussianity of interference) would be highly suboptimal. In Section 3.2, we will deliberate on a low-complexity IA receiver which exploits interference structure in the detection of desired stream.

**2.6.4. Extension to Four Transmit Antennas.** In the case of 4 available transmit antennas, the algorithm described above can be straightforwardly extended. The main difference is in the scheduling, where we pair two users with the highest chordal distance of their respective precoders.

### 3. Receiver Design and Link-Level Studies

This section highlights performance of various receivers for MU-MIMO transmission in LTE systems. Main challenges for an MU-MIMO receiver implementation include fast channel estimation and equalization, reliable multi-user interference cancellation, and complexity issues. The detection method implemented plays a significant role in the resulting performance of MU-MIMO systems, and the main problem leading to the notion of infeasibility of MU-MIMO mode in LTE is the receiver structure employed by the UE being unaware of the interference created by the signal for the other UE. Although the scheduling algorithm discussed in Section 2.6 minimizes the interference based on the geometrical alignment of the channels and the precoders, the residual interference is still significant. Gaussian assumption of this significant interference and the subsequent employment of conventional single-user detectors in this scenario would be highly suboptimal thereby leading to significant degradation in the performance.

**3.1. Receiver Overview.** Maximum likelihood (ML) detection is optimal but exponentially complex as the number of antennas or the size of transmission alphabet increases. In descending order of complexity, a number of suboptimal methods range from the successive interference cancellation (SIC) to the simple linear detectors. Nonlinear algorithms, such as decision feedback-based [22] or tree-based detectors [23], perform near the optimum, but still at the expense of a high complexity. Linear detectors, for example, zero-forcing (ZF) or minimum mean square error (MMSE) criteria, are considerably less complex than ML, but these detectors can suffer a significant performance loss in fading channels in particular in correlated channels [24]. This class of linear detectors also includes the interference rejection combiner (IRC) studied in [25] as a special case. These algorithms are as such readily applicable to LTE systems.

**3.2. Low-Complexity Interference-Aware Receiver.** Another approach for robust LTE DL detection is the low-complexity IA receiver proposed in [26]. This receiver exploits the structure of the residual interference rather than assuming it to be Gaussian in the detection process. In addition to this exploitation, this receiver reduces the system detection complexity by one complex dimension and is thus also applicable to single antenna UEs, which do not possess spatial degrees of freedom to cancel or attenuate the interference via ZF

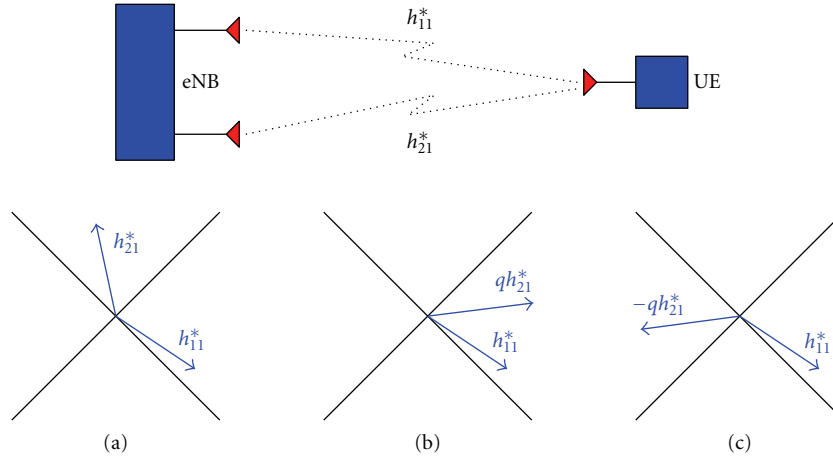


FIGURE 1: (a) shows the original channel from eNB to UE, while (b) shows the effective channel of desired signal and (c) shows the effective channel of interference of UE.

or MMSE filters. This low-complexity receiver being based on the MF outputs and devoid of any division operation is suitable for implementation in the existing hardware [27].

A performance comparison of the IA receiver with a standard (interference *unaware*) receiver for TM5 is given in Figure 2. For comparison, we also consider fallback transmit diversity (TM2) and closed-loop SU-MIMO schemes (TM6). We consider ideal OFDM system (no intersymbol interference (ISI)) and analyze the system in the frequency domain where the channel has *iid* complex Gaussian matrix entries with unit variance and is independently generated for each channel use. We assume no power control in MU-MIMO mode, so two UEs have equal power distribution. It is assumed that the UE knows its own channel from the eNB, so in MU-MIMO mode, UE can find the effective channel of interference based on the fact that the eNB schedules second UE on the same RE which has requested  $180^\circ$  out-of-phase precoder. Note that the MCS for a particular user is the same in each set of simulations. So where one UE is served with a particular MCS in TM6 or TM2, two UEs are served with the same MCS in MU-MIMO (TM5) mode thereby doubling the sum spectral efficiency.

However, the prerequisites of this IA receiver are the knowledge of interference channel and its constellation. Though the scheduling strategy described in Section 2.6 enables the UE to find the effective interference channel (product of interference precoder and own channel), the information regarding the interfering constellation is still eluded due to the DCI formats in LTE do not allow the transmission of this information to the UE. The question is how much sensitive this IA receiver structure is to the knowledge of interfering constellation? To this end, we propose a blind IA receiver in the Appendix which is aware of the interference channel but is unaware of the interfering constellation.

In Figure 3, we look at the sensitivity of the IA detector to the knowledge of the constellation of interference for MU-MIMO mode in LTE. The simulation settings are the same except that we additionally consider the case when UE has no knowledge of the constellation of interference and

thus employs the blind receiver which assumes the unknown interference to be from 16QAM. For comparison purposes, we also consider the cases once UE assumes the unknown interference to be from QPSK and 64QAM. The results show that there is negligible degradation in the performance of the system once the blind IA receiver is employed by the UE which assumes interference to be from 16QAM. This behavior is attributed to the fact the postulation of 16QAM not only captures the effect of four quadrants of QPSK constellation points but also encapsulates the spread of 64QAM constellation points in each quadrant thereby leading to a reasonable compromise.

**3.3. Performance and Complexity Study.** The performance and complexity study is split into two parts. First, we give a brief performance comparison of different receiver architectures in the case of dual antenna eNBs and dual antenna UEs. Secondly, we look at the IA detector [26] in more detail and in the case of dual-antenna eNBs and single-antenna UEs. In both cases, we assume optimal scheduling of users according to Section 2.6.

In this study, we compare IRC studied in [25], the IA detector from [26], and a low-complexity, single-user, linear MMSE (LMMSE) detector. The effect of feedback delay, channel estimation, and spatial correlation has been considered in the investigation. The downlink MU-MIMO LTE Release 8 system investigated is described in Section 2.3. For the link-level evaluation, the parameters defined in Table 3 have been assumed. Due to the straightforward implementation, Least-Squares (LS) channel estimation technique has been applied in investigation.

The results are shown in Figures 4–6. Block error rate (BLER) is presented as a function of the average SNR in dB. For comparison, LTE TM4, SU-MIMO with the ratio of PDSCH (Physical Downlink Shared Channel) EPRE (Energy Per Resource Element) to cell-specific RS EPRE of  $-3$  dB is shown as a reference scenario.

Figure 4 illustrates the performance of all considered detectors for QPSK 1/3, 16QAM 1/3 and 64QAM, 3/4 in

TABLE 3: Basic LTE Parameters Used in the Simulations.

Parameters	Settings
Test scenario	3GPP Macrocell case 1, 19 sites, 57 cells with 3 center cells simulated
Number of UEs	20 UEs per cell and all 20 UEs are semistatically allocated in MU-MIMO mode when MU-MIMO transmission is configured
Carrier frequency and simulated bandwidth	10 MHz bandwidth centered at 2 GHz
Packet scheduling	Proportional fair in both time and frequency domains
1st BLER target	10%
Tx and Rx	$2 \times 2$ and $4 \times 2$ MIMO with SU and MU configured transmission scheme
Tx Correlation	Uncorrelated with $4\lambda$ Tx antennas separation and $15^\circ$ azimuth spread Correlated with $0.5\lambda$ Tx antennas separation and $8^\circ$ azimuth spread
MU-MIMO precoding	Unitary precoder as used in SU-MIMO LTE Release 8
Minimum supported datarate in MU-MIMO mode	64 kbps
$T_{\min}$ UE MU Receiver type	LMMSE, IRC, and IA max-log MAP
Feedback type	Per subband CQI and wideband PMI feedback(one PMI for the whole bandwidth)
Feedback delay	0 TTI and 8 TTI delay
Channel models	Urban microchannel model (uncorrelated) and urban macro (correlated)

uncorrelated channels. The performance of the LMMSE detector degrades with increasing modulation order. For QPSK, IRC slightly outperforms IA max-log MAP (Maximum A Posteriori) detector. However, for 64QAM IA significantly outperforms IRC by almost 5 dB at  $10^{-2}$  BLER. This can be explained by the fact that IA detector exploits not only the interference structure but also performs joint detection as it is aware of the modulation from the interfering user.

The joint effect of feedback delay and channel correlation is illustrated for 16QAM and IA detectors in Figures 5 and 6. In uncorrelated channels (Figure 5), the feedback delay results in up to 2 dB loss at  $10^{-2}$  BLER. However, in the case of high channel correlation, the corresponding performance is reduced by up to 5 dB at  $10^{-2}$  BLER for feedback delay of 8 TTIs (transmit time interval) as shown in Figure 6.

The results shown here demonstrate the possible gains of IA receivers and indicate that the IA type of receivers are good candidates for the practical implementation in MU-MIMO LTE systems. It has been shown that one can obtain the best overall performance with the IA max-log MAP detector if the modulation of the paired UEs is known. However, additional control information bits dedicated to this modulation update may not be desirable as they will increase the downlink overhead and not comparable with the current standardization. By doing a smart scheduling, it is possible to indicate what type of modulation is used for the paired UEs without having dedicated overhead bits for this purpose. The UEs are always informed which MCS will be applied to the next transmitted data packet. In the pairing and selection process, we can then select or force the secondary UEs to have the same modulation as the primary one. To see how often we can actually perform the scheduling of the UE pair having the same modulation, the statistic of the scheduled MU-MIMO UEs pair with their corresponding MCSs is presented in Section 4.2.

## 4. System Level Performance

**4.1. Channel Modeling.** Due to its key role in system performance, the propagation channel needs to be accurately modeled. Proper correlation modeling is critical for MU-MIMO performance assessment. The most advanced models proposed so far are geometry-based stochastic channel models (GSCM), like the WINNER II model [28]. These models explicitly model the geometry of the scenario by choosing random scatterer locations according to some prespecified distribution and might incorporate large-scale fading effects into the channel realizations. When considering a complex scenario, the models inherently take antenna patterns, relative transmitter-receiver locations, angles, and so forth into account. Hence, the correlation matrices become truly UE dependent and time varying which is in accordance with measurement results. In addition, the WINNER II might account for a distance-dependent correlation between the large-scale fading parameters experienced by different terminals situated in the same geographical area.

**4.2. Spatial MU-Packet Scheduler (MU-PS) in LTE Release 8.** The packet scheduler for SU-MIMO transmission is often carried out in two phases: time domain packet scheduler (TDPS) and frequency domain packet scheduler (FDPS). An overview of this TD-FD PS framework in downlink LTE system can be found, for example, in [29, 30]. When MU-MIMO transmission scheme is configured, the UE can be scheduled in SU-MIMO (Rank 1) mode or MU-MIMO mode depending on whether the set multi-user UE pairing condition(s) is (are) met or not. For the pairing purpose, the UEs are classified into primary UEs and candidate UEs [8]. To comply as much as possible with the SU-MIMO mode, the primary UEs are defined as the UEs scheduled for transmission using the same SU-MIMO PS mechanism. The

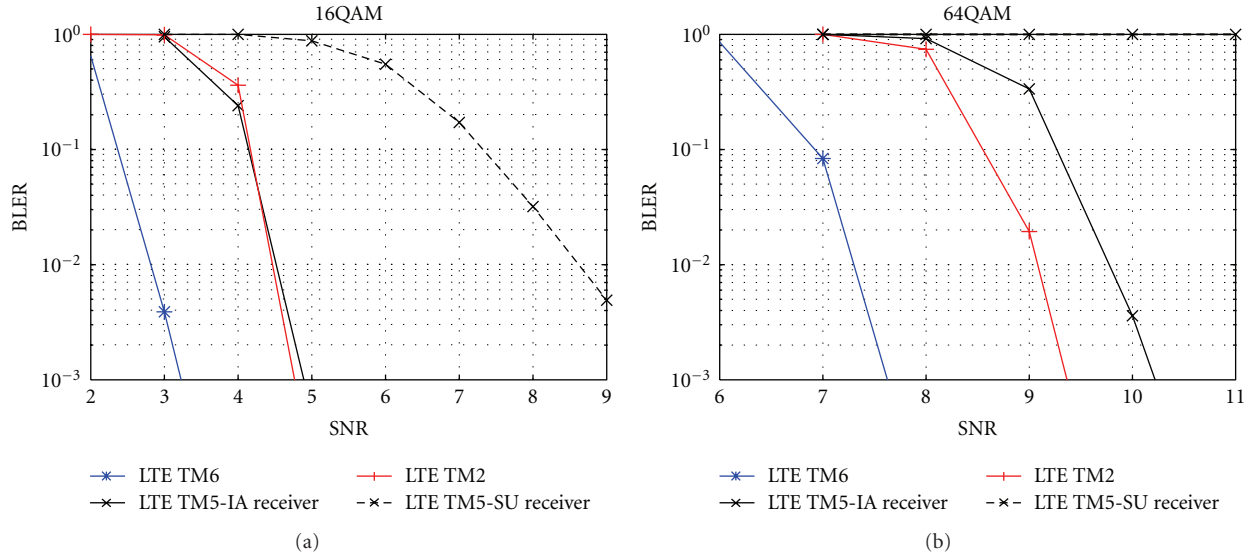


FIGURE 2: BLER versus SNR (dB) comparison of a single-user (SU) receiver and the IA receiver in TM5. The performance of TM6 and TM2 is also shown for comparison. 3GPP LTE rate 1/3 turbo code (punctured to rare 1/2) with 16QAM (a) and 64QAM (b) modulation is used. Both eNB and UE have two antennas, and the channel is i.i.d. Rayleigh fading.

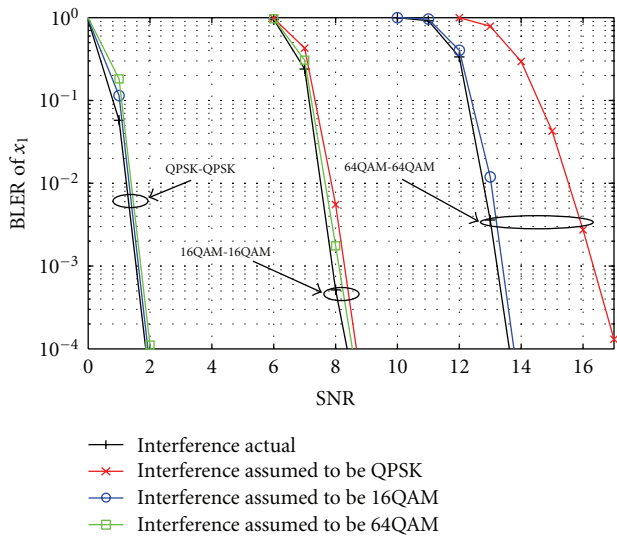


FIGURE 3: BLER versus SNR (dB) of the blind IA for three different constellation orders (e.g., QPSK-QPSK indicates that both  $x_1$  and  $x_2$  are QPSK). “Interference actual” implies the case once UE knows the constellation of interference ( $x_2$ ).

MU-candidate UEs are all UEs with the first transmission (1st Tx). This means UEs with retransmission (2nd Tx) will not be selected as the candidate UEs. This restriction is made in order to facilitate the implementation of Hybrid automatic repeat request (HARQ) procedures where certain number of RBs should be reserved for the retransmissions [29]. By not allowing the 2nd Tx UEs to be candidate UEs, we can make sure that they will be allocated the resource and scheduled as in the SU-MIMO configuration. For each PRB, from the list of MU-candidate UEs, we try to find the best UE to pair

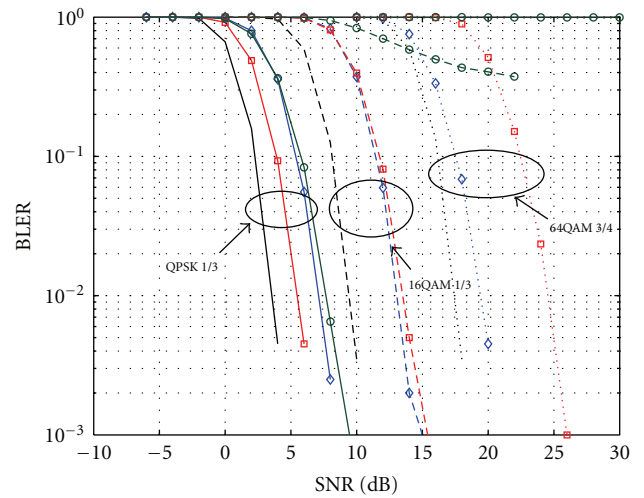


FIGURE 4: BLER versus SNR [dB] performance of MU-MIMO receivers for various modulation orders, urban micro (uncorrelated), 30 km/h, no feedback delay, LS-channel estimation. Line legend: black solid: TM4, SU-MIMO, red  $\square$ : IRC, blue  $\diamond$ : max-log MAP, green  $\circ$ : LMMSE.

with the primary UE. The criterion for selection is that the candidate UE should have an assigned precoder orthogonal to that of the primary UEs. This condition is applied to make sure that the UEs would not cause too much multi-user interference (MUI) to each other. To avoid scheduling the UEs at the cell edge into MU-MIMO mode, the predicted throughput of both the primary UE and the candidate UEs at the considered PRB should be larger than a threshold  $T_{\min}$ . The third requirement is that the candidate UE together with the primary UE should have the sum PF (Proportional Fair)



metrics in MU mode larger than that of the primary in SU mode. Normally, we have a list of candidate UEs that meet these requirements. From this list, the candidate UE that has the highest PF metric in MU mode will be finally paired with the primary UEs and set to MU transmission mode. If none of the candidate UEs meet the first three requirements, the primary UE will transmit in SU mode as normal.

According to LTE Release 8 specification, the UEs are assumed to be semistatically allocated into MU-MIMO mode. In the MU-MIMO mode (Mode 5 [13]), the current control signaling of MU-MIMO parameters is the DCI format 1D. With this 1D DCI format, the UEs assume that an eNB transmission on the PDSCH would be performed on one layer [13]. There is one additional bit to indicate the power sharing/offset and therefore imply the transmission mode of the UEs, for example, SU-MIMO mode or MU-MIMO mode. Due to this specification, the UE scheduled in the SU-MIMO will not use the rank adaptation and only be transmitted in the single-stream mode.

**4.3. Performance of LTE Release 8 MU-MIMO.** Early evaluations for the LTE  $2 \times 2$  MU-MIMO schemes employing various practical precoding approaches (unitary or ZF) and receiver types have disclosed gains over SU-MIMO of up to 20% only in scenarios with high transmit correlation [8]. The precoder granularity was shown to have impact mostly in low-medium transmit correlation scenarios. These conclusions were later confirmed by more extensive investigations, in, for example, [4, 6, 7].

To give an idea on the performance of LTE Release 8 MU-MIMO system, here we provide the system level results of  $2 \times 2$  and  $4 \times 2$  MU-MIMO configurations. The performance of corresponding SU-MIMO systems is also illustrated as a baseline. To comply with the Release 8 specification, the CQI/PMI feedback scheme with per-subband CQI and wideband PMI as reported from the UEs was selected [13]. To make a fair comparison, this feedback scheme was applied for both the SU-MIMO and MU-MIMO transmission configurations. The major input parameters for the simulations are shown in Table 3.

Figure 7 illustrates the distribution of the user throughput for  $4 \times 2$  MIMO with SU and MU transmission configuration. The same trend is observed for the  $2 \times 2$  MIMO setting, and therefore the distribution of the user throughput for this case is not shown. The cell average throughputs for  $2 \times 2$  and  $4 \times 2$  MIMO systems with SU and MU transmission configuration are illustrated in Figure 8. It is observed that with a higher Tx correlation the performance of both SU-MIMO and MU-MIMO is better as compared with the low Tx correlation scenario. This behavior can be explained by the use of wideband PMI. In the uncorrelated Tx antennas scenario, using wideband PMI is not optimum as the fading channel varies quite a lot within the transmission bandwidth used. This leads to a degradation in the performance. On the contrary, when the Tx antennas are correlated, a single wideband PMI represents the optimal precoder for the whole transmission bandwidth. In this case, using either wideband PMI or subband PMI will not change the performance picture.

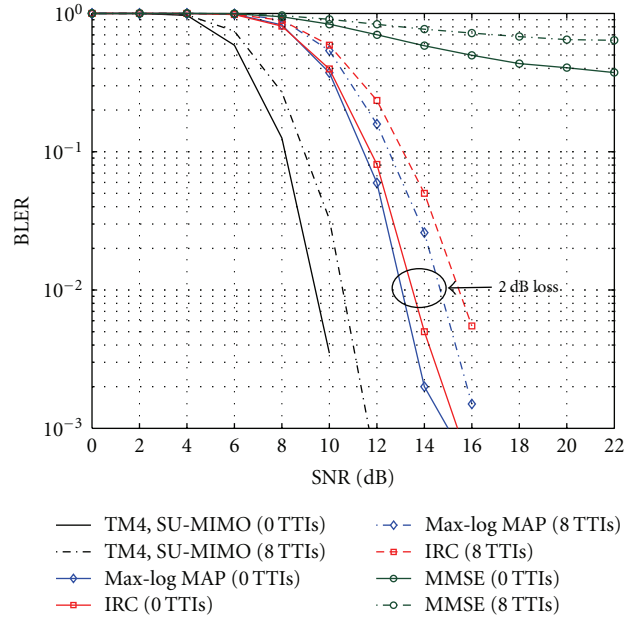


FIGURE 5: BLER versus SNR (dB) performance of MU-MIMO receivers for 16QAM modulation, urban micro, 30 km/h, LS-channel estimation, and feedback delay.

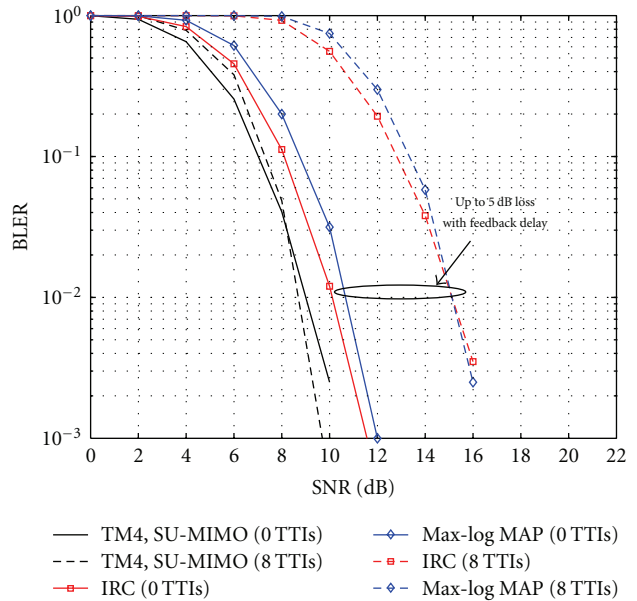


FIGURE 6: BLER versus SNR (dB) performance of MU-MIMO receivers for 16QAM modulation, urban macro, 30 km/h, LS-channel estimation, and feedback delay.

From the cumulative distribution function of the user throughput, it is observed that the 95% ile (peak) user throughput of the MU-MIMO system is lower than that of the SU-MIMO system. At the 5% ile (cell edge) user throughput there is no difference in the performance of MU-MIMO system and SU-MIMO system. This behavior comes from the fact that in the MU-MIMO PS we try not to schedule cell-edge UEs in MU-MIMO mode Section 4.2.

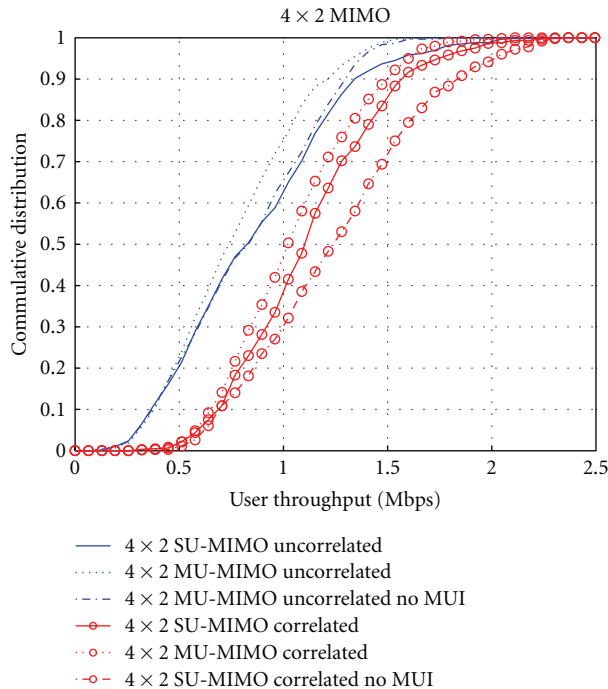


FIGURE 7: Distribution of the user throughput and the average cell throughput for  $4 \times 2$  MIMO setting.

For both  $2 \times 2$  MIMO and  $4 \times 2$  MIMO settings and in both uncorrelated and correlated Tx antennas scenarios, with full multi-user interference, the MU-MIMO system performs worse than the SU-MIMO system with respect to the average cell throughput. Changing the Tx antenna correlation condition, from uncorrelated to correlated, there is an improvement in the average cell throughput of MU-MIMO system, but the enhancement is marginal. The loss in the average cell throughput for  $2 \times 2$  MU-MIMO system and  $4 \times 2$  MU-MIMO system as compared with the corresponding SU-MIMO system is  $-7\%$  and  $-6\%$ , respectively.

For Release 8 UE, it is possible to implement a blind receiver structure as proposed in the Appendix. Figure 3 shows that our proposed blind receiver can work well for all combinations of the modulation order of the MU-MIMO UE pairs except the 64QAM-QPSK combination. In Figure 9, we show the statistics of the scheduled MU-MIMO UEs pair with their corresponding modulation order. It can be seen that up to 40% of the scheduled MU-MIMO pairs have the same modulation order (2-2) QPSK-QPSK, (4-4) 16QAM-16QAM, and (6-6) 64QAM-64QAM. In max 20% of the cases, the modulation order of the paired MU UEs is (6-2, 2-6) 64QAM-QPSK. Therefore, we can safely avoid scheduling UE pairs that have this combination of modulation order.

Based on these observations, we further assume a perfect interference canceling algorithm as upper bound for the practical performance of the blind receiver structure as proposed in the Appendix. Figures 7 and 8 show the system level results obtained under these receiver assumptions. In uncorrelated Tx scenario, even with perfect multi-user interference cancelation, the performance of MU-MIMO system

is inferior to that of the SU-MIMO system. This indicates that one should not use MU-MIMO in an uncorrelated Tx scenario. In a correlated Tx scenario,  $2 \times 2$  MU-MIMO system and  $4 \times 2$  MU-MIMO system obtain a gain in the average cell throughput of 3% and 11%, respectively.

The CQI/PMI feedback scheme used for the results presented in Figures 7 and 8 was limited to the specifications of LTE Release 8. More features are now investigated and proposed in LTE-Advanced standardization, which can facilitate the optimal MU-MIMO transmission and reception. The next section explores some of the potential improvements to be introduced.

#### 4.4. LTE-Advanced Enhancements

**4.4.1. Specific CQI and PMI.** Using the SU-MIMO codebook for MU-MIMO transmission may not fully utilize the multi-user diversity. This is because the SU-MIMO codebook is designed to optimize the performance of a single user, while the additional degree of freedom in the spatial domain one can obtain in the MU-MIMO transmission is not fully taken into consideration. Therefore, it could be beneficial if there is a separated codebook designed specifically for MU-MIMO transmission mode. The multigranular precoder is expected to boost the performance of MU-MIMO system performance as described in [31–33]. Of course, this could raise concern on the increased feedback overhead since an additional MU-MIMO precoder needs to be feedback in parallel with the normal SU-MIMO precoder. Another proposed solution is to report the CQI/PMI separately for SU-MIMO and MU-MIMO transmissions [34, 35]. In addition to the normal SU CQI/PMI feedback, UE capable of receiving MU-MIMO reception could report an additional best companion UE PMI and the expected CQI with that setting. To reduce the feedback overhead, only the difference ( $\Delta$ ) between the MU-CQI and SU-CQI is fed back as extra information. These schemes allow for a dynamic switching between SU and MU modes. One of the drawbacks of these types of proposals is that more feedback overhead is introduced. Moreover, if the paired UEs are restricted to have the same precoding as the best companion precoding, then the number of potential UEs available for pairing at the eNB will be very limited. This could significantly reduce the number of UEs scheduled in MU-MIMO mode and thereby prohibit cell level of the performance gain from using MU-MIMO transmission.

**4.4.2. Link Adaptation and Scheduling.** Although the outer loop link adaptation [36, 37] can help to adjust the estimated MCS for SU-MIMO and compensate for systematic CQI estimation errors, for MU-MIMO in particular, the mismatch between the estimated MU-MIMO CQI and the true channel CQI could still significantly degrade the system performance. For example, the mismatch in the estimated MU-MIMO CQI could lead to a wrong MU-MIMO pairing decision as well as incorrect assignment of the MCS. However, as the UE has no knowledge of the other UE it will be paired with, it is a challenge to estimate the MU-MIMO CQI with a high degree

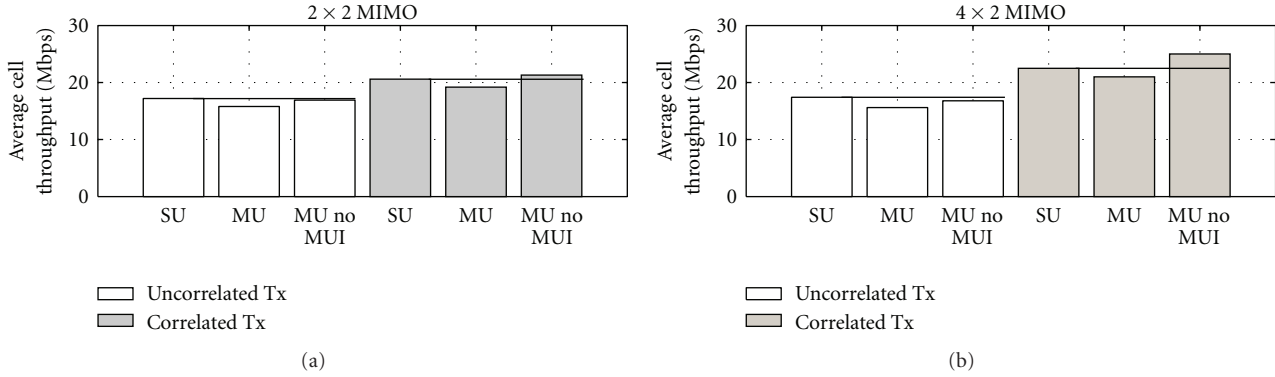


FIGURE 8: The average cell throughputs for  $2 \times 2$  MIMO and  $4 \times 2$  MIMO settings.

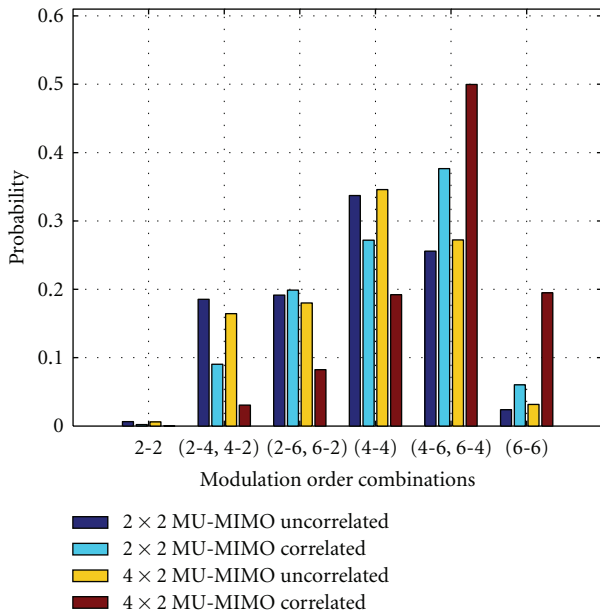


FIGURE 9: Distribution of the combination of the modulation order observed at scheduled MU UEs.

of accuracy. Currently, the most common way of estimating the MU-MIMO CQI is to estimate it from the single-stream SU-MIMO CQI reported by the UE with some offset. Particularly for  $2 \times 2$  MU-MIMO, the offset is around 4.7 dB to account for the power sharing of the two UEs scheduled on the same PRB and the MU interference. The offset value should be differently set for different transmission schemes, for example, orthogonal unitary precoder or ZF. This is because the unitary precoder is already normalized, so that it has norm one. The difference between the SU-MIMO and MU-MIMO comes mainly from the transmission power to the UE in each mode and the MU interference. Meanwhile for ZF, the mismatch between the estimates of MU-MIMO CQI also comes from the fact that the precoder used in the estimation of the SU-MIMO CQI at the UE side is totally different from the actually used transmit ZF precoder at the eNB side.

With the introduction of the DM-RS in LTE Advanced, as the multi-user precoded signals can be estimated at the UE, it is possible to implement a better performing LMMSE receiver with a better multi-user interference covariance matrix estimation.

MU-MIMO scheduling is very much dependent on how much information on the channel can be feedback by the UEs to the serving eNB. There is therefore tradeoff in the performance improvement and the feedback overhead. Currently, in LTE Release 8, the UEs are semistatically allocated to MU-MIMO mode. It means that the UE can not switch from MU-MIMO transmission configuration to SU-MIMO (Rank > 1) transmission configuration between subframes. As mentioned in Section 4.2, together with the specified DCI format, these rules limit the UE comparability in using rank adaptation when it is not scheduled in MU-MIMO mode. This issue is expected to be solved in LTE Advanced when an additional transmission mode (Mode 9) and new DCI format are introduced. This mode would allow for a dynamic switching between SU-MIMO and MU-MIMO and support an SU-MIMO up to rank 8 [18].

### 5. Conclusions

This paper provides a detailed overview of the MU-MIMO schemes encountered in 3GPP standardization, from a unique mode in LTE Release 8 to more advanced possibilities offered by LTE Advanced. Moreover, a new scheduling algorithm based on the geometrical alignment of interference at the base station is proposed. This algorithm minimizes the effective interference seen by each UE.

Various receiver structures are studied. Their performance is assessed in different scenarios at link level. The results shown in this paper have demonstrated the possible gains of IA receivers and indicate that these types of receivers are good candidates for the practical implementation in MU-MIMO LTE systems. However, open research problems still remain. More advanced channel estimation, UE mobility, higher number of transmit and receive antennas, and type of feedback need to be investigated in order to get an overall performance picture of investigated receivers. It may be

noted that these issues have been addressed in SAMURAI, and the outcomes will be published at a later date.

System level simulations for LTE Release 8 are presented and analyzed. It is notably highlighted that for both SU-MIMO and MU-MIMO scenarios better performance is obtained in scenarios with higher Tx correlation than scenarios with low Tx correlation. Interestingly, it is also shown that in terms of average cell throughput, MU-MIMO offers superior performance with respect to SU-MIMO only in correlated scenarios. Furthermore, this gain is shown to be marginal. This disappointing result originates from the limited MU-MIMO features included in Release 8. Hence, proposals considered in LTE-Advanced standardization to better exploit the MU-MIMO potential are thus discussed. They consist in MU-specific CQI and PMI as well as enhanced link adaptation and scheduling.

## Appendix

We describe an extension to the IA receiver proposed in [26] that does not know the interfering constellation.

The max-log MAP bit metric for bit  $b$  of  $x_1$  is given as [38]

$$\Lambda_1^i(y_1, b) \approx \min_{x_1 \in \mathcal{X}_{1,b}^i, x_2 \in \mathcal{X}_2} \left| y_1 - \mathbf{h}_1^\dagger \mathbf{p}_1 x_1 - \mathbf{h}_1^\dagger \mathbf{p}_2 x_2 \right|^2, \quad (\text{A.1})$$

where  $\mathcal{X}_{1,b}^i$  denotes the subset of the signal set  $x_1 \in \mathcal{X}_1$  whose labels have the value  $b \in \{0, 1\}$  in the position  $i$ . We now expand the bit metric which can be rewritten as

$$\begin{aligned} \Lambda_1^i(y_1, b) \approx & \min_{x_1 \in \mathcal{X}_{1,b}^i, x_2 \in \mathcal{X}_2} \left\{ \left| \mathbf{h}_1^\dagger \mathbf{p}_1 x_1 \right|^2 - 2(y_{1, \text{MF}} x_1^*)_R \right. \\ & + \left| \mathbf{h}_1^\dagger \mathbf{p}_2 \right|^2 x_{2,R}^2 - 2|\psi_A| |x_{2,R}| \\ & \left. + \left| \mathbf{h}_1^\dagger \mathbf{p}_2 \right|^2 x_{2,I}^2 - 2|\psi_B| |x_{2,I}| \right\}, \end{aligned} \quad (\text{A.2})$$

where  $y_{1, \text{MF}} = y_1(\mathbf{h}_1^\dagger \mathbf{p}_1)^*$  and  $y_{2, \text{MF}} = y_1(\mathbf{h}_1^\dagger \mathbf{p}_2)^*$  are the outputs of MF. Note that subscripts  $(\cdot)_R$  and  $(\cdot)_I$  indicate real and imaginary parts, respectively. We have introduced two more notations which are given as

$$\begin{aligned} \psi_A &= \rho_{12,R} x_{1,R} + \rho_{12,I} x_{1,I} - y_{2, \text{MF},R}, \\ \psi_B &= \rho_{12,R} x_{1,I} - \rho_{12,I} x_{1,R} - y_{2, \text{MF},I}, \end{aligned} \quad (\text{A.3})$$

where  $\rho_{12} = (\mathbf{h}_1^\dagger \mathbf{p}_1)^* \mathbf{h}_1^\dagger \mathbf{p}_2$  is the cross correlation between the two coefficients. For the minimization of the bit metric, the values of  $x_{2,R}$  and  $x_{2,I}$  need to be in the opposite directions of  $\psi_A$  and  $\psi_B$  which explains the terms  $-2|\psi_A| |x_{2,R}|$  and  $-2|\psi_B| |x_{2,I}|$ .

UE needs to know the constellation of  $x_2$  to compute (A.2). Here, we propose that UE assumes interference ( $x_2$ ) to be from 16QAM. As LTE specifications [16] include only three constellations, that is, QPSK, 16QAM, and 64QAM, so assuming interference to be from 16QAM is a reasonable compromise. It would not only capture the effect

of four quadrants of QPSK constellation points but will also encapsulate the spread of 64QAM constellation points in each quadrant. As the values of  $x_{2,R}$  and  $x_{2,I}$  for the case of 16QAM are  $[\pm(\sigma_2/\sqrt{10}) \pm (3\sigma_2/\sqrt{10})]$ , so the magnitudes of  $x_{2,R}$  and  $x_{2,I}$  which minimize the bit metric (A.2) are given as

$$\begin{aligned} |x_{2,R}| &= \sigma_2 \frac{1}{\sqrt{10}} \left( 2 + (-1)^{I(|\psi_A| < \sigma_2^{(2|\mathbf{h}_1^\dagger \mathbf{p}_2|^2/\sqrt{10})})} \right), \\ |x_{2,I}| &= \sigma_2 \frac{1}{\sqrt{10}} \left( 2 + (-1)^{I(|\psi_B| < \sigma_2^{(2|\mathbf{h}_1^\dagger \mathbf{p}_2|^2/\sqrt{10})})} \right), \end{aligned} \quad (\text{A.4})$$

and  $I(\cdot)$  is the indicator function defined as

$$I(a < b) = \begin{cases} 1 & \text{if } a < b, \\ 0 & \text{otherwise.} \end{cases} \quad (\text{A.5})$$

So, the bit metric for blind receiver is written as

$$\begin{aligned} \Lambda_1^i(y_1, c_{k'}) \approx & \min_{x_1 \in \mathcal{X}_{1,c_{k'}}^i} \left\{ \left| \mathbf{h}_1^\dagger \mathbf{p}_1 x_1 \right|^2 - 2(y_{1, \text{MF}} x_1^*)_R \right. \\ & - 2|\psi_A| |x_{2,R}| + \left| \mathbf{h}_1^\dagger \mathbf{p}_2 \right|^2 |x_{2,R}|^2 \\ & \left. - 2|\psi_B| |x_{2,I}| + \left| \mathbf{h}_1^\dagger \mathbf{p}_2 \right|^2 |x_{2,I}|^2 \right\}, \end{aligned} \quad (\text{A.6})$$

where  $|x_{2,R}|$  and  $|x_{2,I}|$  are given by (A.4).

## Acknowledgment

The research work leading to this paper has been partially funded by the European Commission under FP7 SAMURAI Project. Further details can be found in <http://www.ict-samurai.eu/>.

## References

- [1] 3G Americas white paper, "3GPP Mobile Broadband Innovation Path to 4G: Release 9, Release 10 and Beyond: HSPA+, SAE/LTE and LTE-Advanced," February 2010, [http://www.4gamerica.org/documents/3GPP\\_Rel-9\\_Beyond%20Feb%202010.pdf](http://www.4gamerica.org/documents/3GPP_Rel-9_Beyond%20Feb%202010.pdf).
- [2] Cisco VNI Forecast, "Cisco Visual Networking Index: Global Mobile data Traffic Forecast Update 2009–2014," Cisco Public Information, February 2010, [http://www.cisco.com/en/US/solutions/collateral/ns341/ns525/ns537/ns705/ns827/whitepaper\\_c11-520862.html](http://www.cisco.com/en/US/solutions/collateral/ns341/ns525/ns537/ns705/ns827/whitepaper_c11-520862.html).
- [3] "EU FP7 Project SAMURAI—Spectrum Aggregation and Multi-User MIMO: Real-World Impact," <http://www.ict-samurai.eu/page1001.en.htm>.
- [4] A. Ghosh, R. Ratasuk, B. Mondal, N. Mangalvedhe, and T. Thomas, "LTE-advanced: next-generation wireless broadband technology," *IEEE Wireless Communications*, vol. 17, no. 3, pp. 10–22, 2010.
- [5] Q. Li, G. Li, W. Lee et al., "MIMO techniques in WiMAX and LTE: a feature overview," *IEEE Communications Magazine*, vol. 48, no. 5, pp. 86–92, 2010.

- [6] K. Kusume et al., "System level performance of downlink MU-MIMO transmission for 3GPP LTE-advanced," in *Proceedings of the IEEE Vehicular Technology Conference-Spring (VTC '05)*, Ottawa, Canada, September 2010.
- [7] A. Farajidana et al., "3GPP LTE downlink system performance," in *Proceedings of the IEEE Global Communications Conference (Globecom '09)*, Honolulu, Hawaii, USA, November-December 2009.
- [8] C. B. Ribeiro, K. Hugl, M. Lampinen, and M. Kuusela, "Performance of linear multi-user MIMO precoding in LTE system," in *Proceedings of the 3rd International Symposium on Wireless Pervasive Computing (ISWPC '08)*, pp. 410–414, Santorini, Greece, May 2008.
- [9] I. Z. Kovács, L. G. Ordóñez, M. Navarro, E. Calvo, and J. R. Fonollosa, "Toward a reconfigurable MIMO downlink air interface and radio resource management: the SURFACE concept," *IEEE Communications Magazine*, vol. 48, no. 6, pp. 22–29, 2010.
- [10] G. Caire and S. Shamai, "On the achievable throughput of a multiantenna Gaussian broadcast channel," *IEEE Transactions on Information Theory*, vol. 49, no. 7, pp. 1691–1706, 2003.
- [11] Q. H. Spencer, A. L. Swindlehurst, and M. Haardt, "Zero-forcing methods for downlink spatial multiplexing in multi-user MIMO channels," *IEEE Transactions on Signal Processing*, vol. 52, no. 2, pp. 461–471, 2004.
- [12] C. B. Peel, B. M. Hochwald, and A. L. Swindlehurst, "A vector-perturbation technique for near-capacity multiantenna multi-user communication—part I: channel inversion and regularization," *IEEE Transactions on Communications*, vol. 53, no. 1, pp. 195–202, 2005.
- [13] 3GPP Technical Specification Group Radio Access Network; Evolved Universal Terrestrial Radio Access (E-UTRA), "Physical Layer Procedures (Release 9)," 3GPP TS36.213 V9.3.0, June 2010.
- [14] 3GPP Technical Specification Group Radio Access Network; Evolved Universal Terrestrial Radio Access (E-UTRA), "Physical Channels and Modulation (Release 9)," 3GPP TS36.211 V9.1.0, March 2010.
- [15] 3GPP Technical Specification Group Radio Access Network, "Requirements for Evolved UTRA (E-UTRA) and Evolved UTRAN (E-UTRAN) (Release 7)," 3GPP TR25.913 V7.3.0, March 2006.
- [16] 3GPP TS 36.211, "Evolved Universal Terrestrial Radio Access (E-UTRA); Physical Channels and Modulation, Release 8, V.8.6.0," 2009.
- [17] 3GPP Technical Specification Group Radio Access Network; Evolved Universal Terrestrial Radio Access (E-UTRA), "Further advancements for E-UTRA physical layer aspects (Release 9)," 3GPP TR36.814 V9.0.0, March 2010.
- [18] 3GPP TSG RAN WG1 #62, "Way Forward on Transmission Mode and DCI design for Rel-10 Enhanced Multiple Antenna Transmission," R1-105057, Madrid, Spain, August 2010.
- [19] 3GPP TSG RAN WG1 #62, "Way forward on 8 Tx Codebook for Release 10 DL MIMO," R1-105011, Madrid, Spain, August 2010.
- [20] 3GPP TSG RAN WG1 #62, "Way Forward on Aperiodic PUSCH CQI modes in Release 10," R1-105058, Madrid, Spain, August 2010.
- [21] S. Sesia, I. Toufik, and M. Baker, *LTE, The UMTS Long Term Evolution: From Theory to Practice*, Wiley, 2009.
- [22] G. J. Foschini, G. D. Golden, R. A. Valenzuela, and P. W. Wolniansky, "Simplified processing for high spectral efficiency wireless communication employing multi-element arrays," *IEEE Journal on Selected Areas in Communications*, vol. 17, no. 11, pp. 1841–1852, 1999.
- [23] Y. Jong and T. Willink, "Iterative tree search detection for MIMO wireless systems," in *Proceedings of the 56th IEEE Vehicular Technology Conference (VTC '02)*, Vancouver, Canada, September 2002.
- [24] H. Artés, D. Seethaler, and F. Hlawatsch, "Efficient detection algorithms for MIMO channels: a geometrical approach to approximate ML detection," *IEEE Transactions on Signal Processing*, vol. 51, no. 11, pp. 2808–2820, 2003.
- [25] Wireless World Initiative New Radio WINNER Project, "D1.4 Initial Report on Advanced Multiple Antenna Systems," D1.4, January 2009.
- [26] R. Ghaffar and R. Knopp, "Interference suppression for next generation wireless systems," in *Proceedings of the 69th IEEE Vehicular Technology Conference (VTC '09)*, Barcelona, Spain, April 2009.
- [27] R. Ghaffar and R. Knopp, "Low complexity metrics for BICM SISO and MIMO systems," in *Proceedings of the IEEE Vehicular Technology Conference (VTC '10)*, Taipei, Taiwan, May 2010.
- [28] P. Kyösti, J. Meinilä, L. Hentilä et al., "WINNER II channel models," ver. 1.1, September 2007 <http://www.ist-winner.org/WINNER2-Deliverables/D1.1.2v1.1.pdf>.
- [29] A. Pokhariyal, K. I. Pedersen, G. Monghal et al., "HARQ aware frequency domain packet scheduler with different degrees of fairness for the UTRAN long term evolution," in *Proceedings of the 65th IEEE Vehicular Technology Conference (VTC '07)*, pp. 2761–2765, April 2007.
- [30] G. Monghal, K. I. Pedersen, I. Z. Kovács, and P. E. Mogensen, "QoS oriented time and frequency domain packet schedulers for the UTRAN long term evolution," in *Proceedings of the 67th IEEE Vehicular Technology Conference (VTC '08)*, pp. 2532–2536, May 2008.
- [31] 3GPP TSG RAN WG1 #61bis, "Multi-granularity codebooks for 4Tx DL MIMO," R1-103480, Dresden, Germany, June-July 2010.
- [32] 3GPP TSG RAN WG1 meeting #61bis, "Double codebook based differential feedback for MU-MIMO enhancement," R1-103449, Dresden, Germany, June-July 2010.
- [33] 3GPP TSG RAN WG1 #61bis, "System-Level Evaluation Results on 8Tx Codebook," R1-103703, Dresden, Germany, June-July 2010.
- [34] 3GPP TSG RAN WG1 #62 Meeting, "Further analysis of companion feedback performance and feedback signalling overhead reduction," R1-092680, Madrid, Spain, August 2010.
- [35] 3GPP TSG RAN WG1 #56 Meeting, "Best Companion reporting for improved single-cell MU-MIMO pairing," R1-090926, Athens, Greece, February 2009.
- [36] H. Holma and A. Toskala, *LTE for UMTS—OFDMA and SC-FDMA Based Radio Access*, Wiley, 2009.
- [37] K. I. Pedersen, G. Monghal, I. Z. Kovács et al., "Frequency domain scheduling for OFDMA with limited and noisy channel feedback," in *Proceedings of the 66th IEEE Vehicular Technology Conference (VTC '07)*, pp. 1792–1796, October 2007.
- [38] G. Caire, G. Taricco, and E. Biglieri, "Bit-interleaved coded modulation," *IEEE Transactions on Information Theory*, vol. 44, no. 3, pp. 927–946, 1998.